Available online at www.sciencedirect.com
SCIENCE DIRECT
Polymer 47 (2006) 1875–1885
polymer
www.elsevier.com/locate/polymer

Synthesis of optically active methacrylic oligomeric models and polymers bearing the side-chain azo-aromatic moiety and dependence of their chiroptical properties on the polymerization degree

L. Angiolini *, T. Benelli, L. Giorgini, E. Salatelli

Dipartimento di Chimica Industriale e dei Materiali and INSTM UdR-Bologna, University of Bologna, Viale Risorgimento 4, 40136 Bologna, Italy

Received 3 November 2005; received in revised form 3 January 2006; accepted 13 January 2006
Available online 7 February 2006

Abstract

Three oligomeric models (dimer, trimer and tetramer) of optically active methacrylic polymers containing in the side-chain the pyrrolidinyl group of one single configuration linked through the nitrogen atom to the azobenzene chromophore and the related homopolymers in a wide range of average polymerization degree ($13 < \bar{X}_n < 70$) and different molecular weight distributions, were synthesized. Their characterization afforded the possibility to investigate the dependence of the properties on the average molecular weight of polymeric derivatives. In particular, the investigation of optical rotation and chiroptical properties by circular dichroism allowed to confirm the conformational origin of chirality in this class of materials as well as to correlate the optical activity to the molecular weight.

Keywords: Chiroptical properties; Chiral azobenzene-containing polymers; Chiral amplification

1. Introduction

Optically active photochromic polymers bearing in the side-chain both a chiral group of one single configuration and the *trans*-azoaromatic moiety with a conjugated electron donor–acceptor system, have received considerable attention for their potential advanced technological applications. Displaying, in fact, both the properties typical of dissymmetric systems [1] (optical activity, absorption of circularly polarized light in the UV–vis spectral region), as well as the features of photochromic materials [2,3] (NLO properties, photoresponsiveness, photorefractivity) they can be proposed as devices for the optical storage of information, waveguides, chiroptical switches, chemical photoreceptors, etc. [4–7].

In this context, we recently reported synthesis and characterization of polymethacrylates bearing a rigid chiral group of one single configuration interposed between the main chain and the *trans*-azoaromatic chromophore [8–12]. The presence of conformational dissymmetry in these systems can be detected by chiroptical techniques, such as circular dichroism (CD), suitable to reveal the existence of chiral perturbation induced by the optically active moieties onto the electronic transitions of the achiral aromatic chromophore. The appearance of remarkable dichroic effects in the absorption region of the azoaromatic chromophore thus allowed to disclose that these macromolecules may assume, in dilute solution, a conformational dissymmetry of one prevailing screw sense. This effect is more evident in polymers bearing a rigid cyclic group, such as (*S*)-2-hydroxy succinimide [10,11] or (*S*)-3-hydroxy pyrrolidine [12] as a chiral spacer, whose CD spectra show strong exciton couplets. The gradual insertion in the main chain of achiral co-units, such as methyl methacrylate [13], however, afforded co-polymeric products exhibiting a progressive decrease of the exciton couplet amplitude. Such a behaviour is the consequence of the reduction of co-operative interactions among the chiral co-units, thus decreasing the conformational homogeneity of the macromolecules and hence the average length of chain sections with a single prevailing chirality.

However, the results suggested that even few adjacent chiral units should be able to produce a remarkable conformational dissymmetry in the macromolecules. Indeed, this has been confirmed by recent studies on the dimeric derivative 2,4-dimethyl-glutaric acid bis(*S*)-3-[1-(4′-nitro-4-azobenzene)-pyrrolidine ester [14], corresponding to the smallest section

* Corresponding author. Tel./fax: +39 051 2093687.
E-mail address: luigi.angiolini@unibo.it (L. Angiolini).

0032-3861/$ - see front matter © 2006 Elsevier Ltd. All rights reserved.
doi:10.1016/j.polymer.2006.01.044

of polymer where interchromophore interactions can be present. The CD spectra collected in several solvents, in fact, showed a strong exciton couplet (about one third of the signal intensity measured for the corresponding polymer), which suggests that chiral interactions between a couple of chromophores in solution are already important and that the optical activity of these materials should be substantially related to relatively short chain sections with conformational dissymmetry of one prevailing screw sense.

To this regard, we have recently synthesized by ATRP [15] a series of optically active methacrylic homopolymers poly[(*S*)-3-methacryloyloxy-1-(4-azobenzene)pyrrolidine] {poly[(*S*)-MAP]} (Fig. 1), with different average polymerization degree (in the range 10–30) and low polydispersity index. The results indicate that the chirality of these macromolecules is due to conformational effects and strongly depends on their chain length.

With the aim to investigate further into this behaviour, we report in the present paper synthesis and characterization of oligomeric models of the above optically active methacrylic homopolymers, such as the dimer, trimer and tetramer. In addition, a novel, extended series of homopolymeric samples with different average molecular weight and polydispersity values has been investigated (Fig. 1).

Thermal properties, electronic spectra and optical activity of the obtained products have been compared with those displayed by the homopolymers poly[(*S*)-MAP] previously obtained by AIBN-initiated polymerization [12] and ATRP [15], as well as by the low molecular weight model compound (*S*)-(+)-3-pivaloyloxy-1-(4-azobenzene)pyrrolidine [(*S*)-PAP] [12] (Fig. 1), representative of the repeating unit of the polymeric derivatives.

2. Experimental

2.1. Physico-chemical measurements

^{1}H and ^{13}C NMR spectra were obtained at room temperature, on 5–10% $CDCl_3$ solutions, using a Varian NMR Gemini 300 spectrometer. Chemical shifts are given in ppm from tetramethylsilane (TMS) as the internal reference. ^{1}H NMR spectra were run at 300 MHz by using the following experimental conditions: 24,000 data points, 4.5-kHz spectral width, 2.6-s acquisition time, 128 transients. ^{13}C NMR spectra were recorded at 75.5 MHz, under full proton decoupling, by using the following experimental conditions: 24,000 data points, 20-kHz spectral width, 0.6-s acquisition time, 64,000 transients. FT-IR spectra were carried out on a Perkin–Elmer 1750 spectrophotometer, equipped with an Epson Endeavour II data station, on sample prepared as KBr pellets.

UV–vis absorption spectra were recorded at 25 °C in the 700–250 nm spectral region with a Perkin–Elmer Lambda 19 spectrophotometer on $CHCl_3$ solutions by using cell path lengths of 0.1 cm.

Concentrations in azobenzene chromophore of about 3×10^{-4} mol L^{-1} were used.

Optical activity measurements were accomplished at 25 °C on $CHCl_3$ solutions ($c\approx0.250$ g dL^{-1}) with a Perkin–Elmer 341 digital polarimeter, equipped with a Toshiba sodium bulb, using a cell path length of 1 dm. Specific and molar rotation values at the sodium D line are expressed as deg dm^{-1} g^{-1} cm^3 and deg dm^{-1} mol^{-1} dL, respectively.

Circular dichroism (CD) spectra were carried out at 25 °C on $CHCl_3$ solutions on a Jasco 810 A dichrograph, using the same path lengths and solution concentrations as for the UV–vis measurements. $\Delta\varepsilon$ values, expressed as L mol^{-1} cm^{-1}

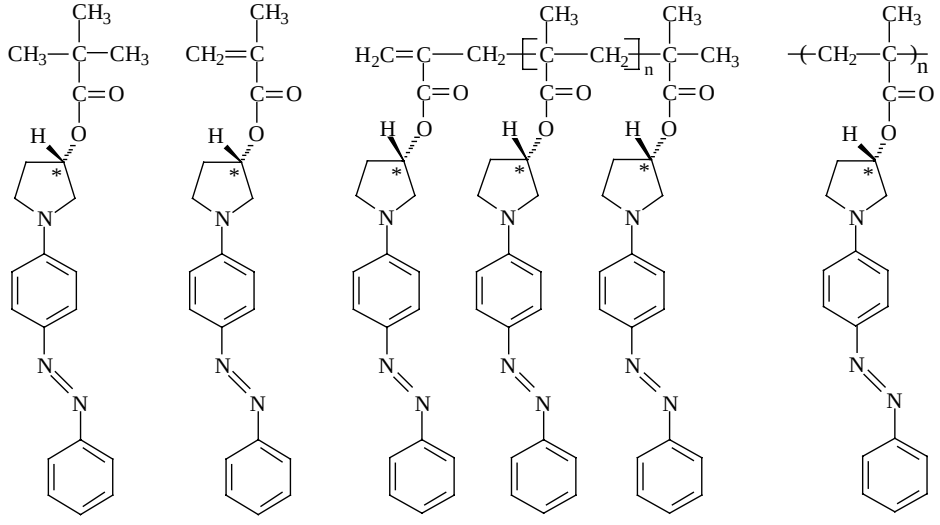

Fig. 1. Chemical structures of model compound (*S*)-PAP, monomer (*S*)-MAP, oligomeric models and the related homopolymer poly[(*S*)-MAP].

were calculated from the following expression: $\Delta\varepsilon = [\Theta]/3300$, where the molar ellipticity $[\Theta]$ in deg cm^2 dmol^{-1} refers to one azobenzene chromophore.

Number average molecular weights of the polymers (M_n) and their polydispersity indexes (M_w/M_n) were determined in THF solution by SEC using HPLC Lab Flow 2000 apparatus, equipped with an injector Rheodyne 7725i, a Phenomenex Phenogel 5-μm MXL column, or a Phenomenex Phenogel 5-μm MXM column, and a UV–vis detector Linear Instrument model UVIS-200, working at 254 nm. Calibration curves for MXL and MXM columns were obtained by using monodisperse polystyrene standards in the range 800–35,000 and 2700–200,000, respectively.

The glass transition temperature values were determined by differential scanning calorimetry (DSC) on a TA Instrument DSC 2920 modulated apparatus at a heating rate of 10 °C/min under nitrogen atmosphere on samples weighing 5–9 mg. Checking of the liquid crystalline behaviour was carried out with an Zeiss Axioscope2 polarising microscope through crossed polarizers fitted with a Linkam THMS 600 hot stage.

The initial thermal decomposition temperature (T_d) was determined on the polymeric samples with a Perkin–Elmer TGA-7 thermogravimetric analyzer by heating the samples in air at a rate of 20 °C/min. Melting points (uncorrected) were determined in glass capillaries on a Büchi 510 apparatus at a heating rate of 1 °C/min.

2.2. Materials

The azoic alcohol (*S*)-(−)-3-hydroxy-1-(4-azobenzene) pyrrolidine [(*S*)-HAP], the monomer (*S*)-(+)-3-methacryloyloxy-1-(4-azobenzene)pyrrolidine [(*S*)-MAP] and the model compound (*S*)-(+)-3-pivaloyloxy-1-(4-azobenzene)pyrrolidine [(*S*)-PAP] were synthesized as previously reported [12].

Chloroform and THF were purified and dried according to the reported procedures [16] and stored under nitrogen.

The solution of the chain transfer complex catalyst, cobalt(II) chelated with 4,7-diaza-2,9-dihydroxyimino-3,8-dimethyldeca-3,7-diene $[Co(II)DDDD\text{-}H]^+CH_3COO^-$, 10^{-3} M in methyl ethyl ketone, was prepared immediately before use as described [17]. The BF_2-bridged dimethylglyoxime cobalt complex $[Co(II)(DHIB\text{–}BF_2)_2(H_2O)_2]$ was prepared as described [18,19] and recrystallized in diethyl ether immediately before use.

2.3. Synthesis of oligomeric models

2.3.1. 2,4-Bis(methoxycarbonyl)-4-methylpent-1-ene (MMA dimer), 2,4,6-tris(methoxycarbonyl)-4,6-dimethylhept-1-ene (MMA trimer) and 2,4,6,8-tetra(methoxycarbonyl)-4,6,8-trimethylnon-1-ene (MMA tetramer)

General procedure. MMA oligomers were prepared with a procedure similar to that one previously reported by Rizzardo and co-workers [20], by fractional distillation under vacuum (0.03 mm Hg) of the oily mixture containing the oligomers produced by radical polymerization of MMA (0.1 mol) in methyl ethyl ketone (40 mL), with AIBN (1% in mol with respect to monomer) as initiator and $[Co(II)DDDD\text{-}H]^+CH_3COO^-$ at a concentration of 2.5×10^{-4} M [17,21] as catalytic chain transfer agent. To obtain a sufficient amount of MMA tetramer, the above procedure was repeated reducing the quantity of cobalt complex to 2.0×10^{-4} M.

Pure MMA dimer (bp 44–45 °C at 0.03 mm Hg) and MMA trimer (bp 101–103 °C at 0.03 mm Hg) were isolated by fractional distillation, the undistilled residual viscous oil, composed of a tetramer-rich fraction with traces of derivatives of higher molecular weight, was purified by column chromatography on SiO_2 (petroleum ether/ethyl acetate 4:1 v/v as eluent) to give the pure MMA tetramer (mp 53–56 °C).

^{1}H NMR characterization data are as follows (atoms labelling as in Fig. 2).

2.3.1.1. MMA dimer. ^{1}H NMR ($CDCl_3$): 6.22 and 5.52 (dd, 2H, $=CH_2$), 3.73 and 3.65 (2s, 6H, $-OCH_3$), 2.61 (s, 2H, B_3 CH_2), 1.17 (2s, 6H, M_4 and M_5 CH_3) ppm.

2.3.1.2. MMA trimer. ^{1}H NMR ($CDCl_3$): 6.20 and 5.50 (dd, 2H, $=CH_2$), 3.73, 3.65 and 3.61 (3s, 9H, $-OCH_3$), 2.55 (s, 2H, B_3 CH_2), 2.10 (dd, 2H, B_5 CH_2), 1.18, 1.06 and 1.00 (3s, 9H, M_4, M_6 and M_7 CH_3) ppm.

2.3.1.3. MMA tetramer. ^{1}H NMR ($CDCl_3$): 6.20 and 5.50 (dd, 2H, $=CH_2$), 3.72, 3.64, 3.62 and 3.60 (4s, 12H, $-OCH_3$), 2.50 (s, 2H, B_3 CH_2), 2.10 (m, 2H, B_5 CH_2), 1.90 (m, 2H, B_7 CH_2),

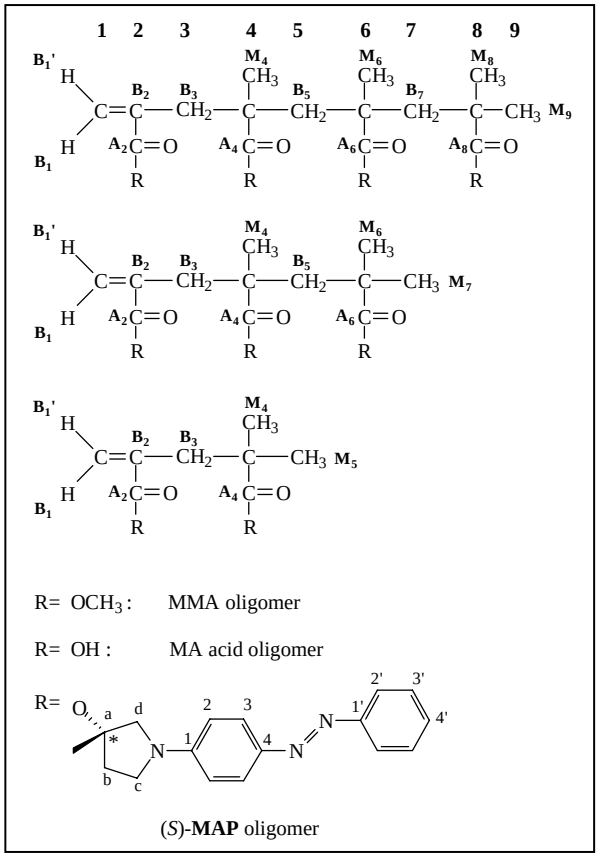

Fig. 2. Atoms labelling of oligomeric derivatives.

1.15, 1.06, 0.97 and 0.94 (4s, 12H, M_4, M_6, M_8 and M_9 CH_3) ppm.

2.3.2. 2,4-Bis(hydroxycarbonyl)-4-methylpent-1-ene acid (MA acid dimer)

A large excess of KOH (180 mmol, 6 equiv. of KOH for 1 equiv. of ester) in water (10 mL) was added to a solution of MMA dimer (15 mmol) in abs. ethanol (19.2 mL) and the mixture, after addition of hydroquinone (0.10 g), was heated at reflux, monitoring the progress of the saponification reaction by FT-IR until the disappearance of the ester absorption at 1730 cm^{-1}, completed after about 1 h. The solvent was then evaporated under reduced pressure and the obtained solid material dissolved in water previously acidified with aq. HCl (pH = 1). The product was finally extracted with diethyl ether, dried with anh. Na_2SO_4 and the organic phase evaporated under reduced pressure to give the MA acid dimer (yield 98%, mp 120–122 °C).

^1H, ^{13}C NMR and FT-IR characterization data are as follows (atoms labelling as in Fig. 2).

^1H NMR ($CDCl_3$/DMSO-d_6 1:1 v/v): 11.20 (s, 2H, OH), 6.22 and 5.60 (dd, 2H, $=CH_2$), 2.60 (s, 2H, B_3 CH_2), 1.17 (2s, 6H, M_4 and M_5 CH_3) ppm.

^{13}C NMR ($CDCl_3$/DMSO-d_6 1:1 v/v): 185.6 (A_4 *C*O), 173.8 (A_2 *C*O), 138.2 (B_2 *C*), 127.5 (=*C*H_2), 42.8 (B_4 *C*), 40.2 (B_3 *C*H_2), 24.9 (M_4 and M_5 *C*H_3) ppm.

FT-IR (KBr): 3440 (ν_{OH}), 2979 (ν_{CH}, aliph), 1707 ($\nu_{C=O}$), 1629 ($\nu_{C=C}$), 1475 (δ_{CH}), 1296 (δ_{C-O}), 1201 (ν_{C-O}) cm^{-1}.

2.3.3. 2,4,6-Tris(hydroxycarbonyl)-4,6-dimethylept-1-ene acid (MA acid trimer)

MA acid trimer was prepared by saponification of MMA trimer using the same procedure above described for MMA dimer. The product was obtained in 98% yield, mp 148–151 °C.

^1H NMR ($CDCl_3$/DMSO-d_6 1:1 v/v): 11.25 (s, 3H, OH), 6.40 and 5.70 (dd, 2H, $=CH_2$), 2.60 (s, 2H, B_3 CH_2), 2.00 (m, 2H, B_5 CH_2), 1.18, 1.06 and 1.00 (3s, 9H, M_4, M_6 and M_7 CH_3) ppm.

^{13}C NMR ($CDCl_3$/DMSO-d_6 1:1 v/v): 185.8 (A_6 *C*O), 184.2 (A_4 *C*O), 173.8 (A_2 *C*O), 136.5 (B_2 *C*), 131.3 (=*C*H_2), 47.8 (B_5 *C*H_2), 45.7 (B_4 *C*), 44.5 (B_3 *C*H_2), 42.2 (B_6 *C*), 30.0 (M_6 *C*H_3), 24.0 (M_7 *C*H_3) and 20.6 (M_4 *C*H_3) ppm.

FT-IR (KBr): 3450 (ν_{OH}), 2982 (ν_{CH}, aliph), 1702 ($\nu_{C=O}$), 1625 ($\nu_{C=C}$), 1480 (δ_{CH}), 1296 (δ_{C-O}), 1195 (ν_{C-O}) cm^{-1}.

2.3.4. 2,4,6,8-Tetra(hydroxycarbonyl)-4,6,8-trimethylnon-1-ene acid (MA acid tetramer)

MA acid tetramer was prepared by saponification of MMA tetramer using the same procedure above described for MMA dimer. The product was obtained in 91% yield, mp not determinable.

^1H NMR ($CDCl_3$/DMSO-d_6 1:1 v/v): 11.10 (s, 4H, OH), 6.22 and 5.60 (dd, 2H, $=CH_2$), 2.60 (s, 2H, B_3 CH_2), 2.05 (m, 2H, B_5 CH_2), 1.90 (m, 2H, B_7 CH_2), 1.15, 1.06, 0.97 and 0.94 (4s, 12H, M_4, M_6, M_8 and M_9 CH_3) ppm.

^{13}C NMR ($CDCl_3$/DMSO-d_6 1:1 v/v): 181.3 (A_8 *C*O), 181.1 (A_6 *C*O), 179.6 (A_4 *C*O), 169.9 (A_2 *C*O), 137.5 (B_2 *C*), 128.5 (=*C*H_2), 51.8 (B_5 *C*H_2), 48.2 (B_4 *C*), 46.4 (B_6 *C*), 44.7 (B_7 *C*H_2), 42.7 (B_3 *C*H_2), 41.4 (B_8 *C*), 30.2 (M_8 *C*H_3), 22.5 (M_9 *C*H_3), 18.9 (M_4 *C*H_3) and 18.2 (M_6 *C*H_3) ppm.

FT-IR (KBr): 3450 (ν_{OH}), 2980 (ν_{CH}, aliph), 1700 ($\nu_{C=O}$), 1620 ($\nu_{C=C}$), 1481 (δ_{CH}), 1261 (δ_{C-O}), 1186 (ν_{C-O}) cm^{-1}.

2.3.5. 2,4-Bis{(S)-(−)-[1-(4-azobenzene)]-3-pyrrolidinoxycarbonyl}-4-methylpent-1-ene [(S)-MAP dimer], 2,4,6-tris{(S)-(−)-[1-(4-azobenzene)]-3-pyrrolidinoxycarbonyl}-4,6-dimethylept-1-ene [(S)-MAP trimer] and 2,4,6,8-tetra{(S)-(−)-[1-(4-azobenzene)]-3-pyrrolidinoxycarbonyl}-4,6,8-trimethylnon-1-ene [(S)-MAP tetramer]

General procedure. To a stirred solution of MA acid oligomer (14.6 mmol) and a molar excess of (*S*)-HAP (2 equiv. of alcohol for 1 equiv. of acid) in CH_2Cl_2 (600 mL), 4-(dimethylamino)pyridinium 4-toluensulfonate (DPTS, 1 equiv. for 1 equiv. of acid) and 1,3 diisopropylcarbodiimide (DIPC, 1.3 equiv. for 1 equiv. of acid) were added under nitrogen flow. The mixture was kept at room temperature under nitrogen flow for some days and the progress of the reaction monitored by thin layer chromatography. The crude product was then repeatedly washed with distilled water and dried with anh. Na_2SO_4. The final purification was performed by column chromatography (SiO_2, $CHCl_3$/EtOAc 4:1 v/v as eluent) followed by crystallization in *n*-pentane. Relevant data for the synthesized products are reported in Table 1.

^1H, ^{13}C NMR and FT-IR characterization data are as follows (atoms labelling as in Fig. 2).

2.3.5.1. (S)-MAP dimer (yield 18%, mp 140–142 °C). ^1H NMR ($CDCl_3$): 7.85 (m, 4H, arom. 2′-H), 7.80 (dd, 4H, arom. *meta* to amino group), 7.50 (m, 4H, arom. 3′-H), 7.30 (m, 2H, arom. 4′-H), 6.60 (dd, 4H, arom. *ortho* to amino group), 6.15 and 5.50 (dd, 2H, $=CH_2$), 5.40 (m, 2H, 3-CH), 3.70–3.40 (m, 8H, pyrrolidine 2- and 5-CH_2), 2.60 (s, 2H, B_3 CH_2), 2.30 (m, 4H, pyrrolidine 4-CH_2) and 1.17 (2s, 6H, M_4 and M_5 CH_3) ppm.

^{13}C NMR ($CDCl_3$): 177.3 (A_4 *C*O), 167.6 (A_2 *C*O), 153.8, 150.1, 144.4 (arom *C*–N=N–*C* and *C*–N–CH_2), 137.7 (B_2 *C*), 130.2 (arom 4′-C), 129.6 (arom 3′-C), 125.8, 122.9 (arom 2′-C and 3-C), 129.2 (=*C*H_2), 112.2 (arom 2-C), 74.4 (CH–O), 54.4 (CH–*C*H_2–N), 46.4 (CH_2–*C*H_2–N), 43.3 (B_4 *C*), 41.4 (B_3 *C*H_2), 31.8 (CH–*C*H_2–CH_2), 25.7 (M_4 *C*H_3) and 25.4 (M_5 *C*H_3) ppm.

FT-IR (KBr): 3061 (ν_{CH}, arom), 2924 and 2852 (ν_{CH}, aliph), 1718 (ν_{CO}, ester), 1635 ($\nu_{C=C}$), 1605 and 1516 ($\nu_{C=C}$, arom),

Table 1
Characterization data of oligomeric models

Samples	Yield (%)	Mp (°C)	$[\alpha]_D^{25}$ [a]	$[\Phi]_D^{25}$ [b]
(*S*)-PAP[c]	53	149–150	+4.0	+14.0
(*S*)-MAP dimer	18	140–142	+43.8	+146.6
(*S*)-MAP trimer	4	135–137	+69.5	+233.1
(*S*)-MAP tetramer	1	n.d.	+110.9	+372.0

[a] Specific optical rotation, expressed as deg dm^{-1} g^{-1} dL.
[b] Molar optical rotation, expressed as deg dm^{-1} mol^{-1} dL and calculated as ($[\alpha]_D^{25}M/100$), where *M* represents the molecular weight of (*S*)-PAP or the molecular weight of one repeating unit of oligomers.
[c] Ref. [12].

1142 (ν_{C-O}), 816 (δ_{CH}, 1,4-disubst. arom ring), 765 and 687 (δ_{CH}, monosubst. arom ring) cm^{-1}.

2.3.5.2. (S)-MAP trimer (yield 4%, mp 135–137 °C). ^1H NMR ($CDCl_3$): 7.85 (m, 6H, arom. 2′-H), 7.80 (dd, 6H, arom. *meta* to amino group), 7.50 (m, 6H, arom. 3′-H), 7.30 (m, 3H, arom. 4′-H), 6.60 (dd, 6H, arom. *ortho* to amino group), 6.15 and 5.50 (dd, 2H, $=CH_2$), 5.40 (m, 3H, 3-CH), 3.70–3.40 (m, 12H, pyrrolidine 2- and 5-CH_2), 2.60 (s, 2H, B_3 CH_2), 2.30 (m, 6H, pyrrolidine 4-CH_2), 2.00 (m, 2H, B_5 CH_2), 1.18, 1.06 and 1.00 (3s, 9H, M_4, M_6 and M_7 CH_3) ppm.

^{13}C NMR ($CDCl_3$): 177.3 (A_6 *C*O), 167.9 (A_4 *C*O), 166.2 (A_2 *C*O), 153.8, 150.1, 144.5 (arom *C*–N=N–*C* and *C*–N–CH_2), 137.8 (B_2 *C*), 130.1 (arom 4′-C), 129.6 (arom 3′-C), 129.2 (=*C*H_2), 125.8, 122.8 (arom 2′-C and 3-C), 112.2 (arom 2-C), 74.4 (CH–O), 54.1 (CH–*C*H_2–N), 46.4 (B_5 *C*H_2), 46.2 (CH_2–*C*H_2–N), 45.7 (B_4 *C*), 43.3 (B_3 *C*H_2), 41.4 (B_6 *C*), 31.8 (CH–*C*H_2–CH_2), 26.2 (M_6 *C*H_3), 25.7 (M_7 *C*H_3) and 25.4 (M_4 *C*H_3) ppm.

FT-IR (KBr): 3060 ($\nu_{CH,}$ arom), 2923 and 2851 (ν_{CH}, aliph), 1718 (ν_{CO}, ester), 1632 ($\nu_{C=C}$), 1605 and 1515 ($\nu_{C=C}$, arom), 1140 (ν_{C-O}), 816 (δ_{CH}, 1,4-disubst. arom ring), 765 and 687 (δ_{CH}, monosubst. arom ring) cm^{-1}.

2.3.5.3. (S)-MAP tetramer (yield 1%, mp not determinable). ^1H NMR ($CDCl_3$): 7.85 (m, 8H, arom. 2′-H), 7.80 (dd, 8H, arom. *meta* to amino group), 7.50 (m, 8H, arom. 3′-H), 7.30 (m, 4H, arom. 4′-H), 6.60 (dd, 8H, arom. *ortho* to amino group), 6.15 and 5.50 (dd, 2H, $=CH_2$), 5.40 (m, 4H, 3-CH), 3.70–3.40 (m, 16H, pyrrolidine 2- and 5-CH_2), 2.60 (s, 2H, B_3 CH_2), 2.30 (m, 8H, pyrrolidine 4-CH_2), 2.05 (m, 2H, B_5 CH_2), 1.90 (m, 2H, B_7 CH_2), 1.15, 1.06 and 0.97 and 0.94 (4s, 12H, M_4, M_6, M_8 and M_9 CH_3) ppm.

^{13}C NMR ($CDCl_3$): 177.4 (A_8 and A_6 *C*O), 167.8 (A_4 *C*O), 166.3 (A_2 *C*O), 153.8, 150.1, 144.5 (arom *C*–N=N–*C* and *C*–N–CH_2), 137.8 (B_2 *C*), 130.1 (arom 4′-C), 129.6 (arom 3′-C), 129.2 (=*C*H_2), 125.8, 122.8 (arom 2′-C and 3-C), 112.2 (arom 2-C), 74.4 (CH–O), 54.1 (CH–*C*H_2–N), 50.9 (B_5 *C*H_2), 46.5 (B_7 *C*H_2), 46.2 (CH_2–*C*H_2–N), 45.7 (B_6 *C*), 45.2 (B_4 *C*), 43.4 (B_3 *C*H_2), 41.2 (B_8 *C*), 31.8 (CH–*C*H_2–CH_2), 26.4 (M_8 *C*H_3), 25.7 (M_9 *C*H_3), 25.4 (M_4 *C*H_3) and 21.7 (M_6 *C*H_3) ppm.

FT-IR (KBr): 3062 (ν_{CH}, arom), 2926 and 2851 (ν_{CH}, aliph), 1718 (ν_{CO}, ester), 1633 ($\nu_{C=C}$), 1605 and 1515 ($\nu_{C=C}$, arom), 1141 (ν_{C-O}), 816 (δ_{CH}, 1,4-disubst. arom ring), 765 and 687 (δ_{CH}, monosubst. arom ring) cm^{-1}.

2.4. Synthesis of poly[(S)-MAP] samples of different average molecular weight

Several methacrylic homopolymeric samples of poly[(*S*)-MAP] with different average molecular weights and polydispersity values were obtained from monomer (*S*)-MAP through two synthetic methods. All the products were characterized by FT-IR, ^1H and ^{13}C NMR.

2.5. Radical polymerization of (S)-MAP in the presence of AIBN (10%wt) and subsequent fractionation

A solution of 1.0 g of monomer in 15 mL of dry THF was introduced into a vial under nitrogen atmosphere, submitted to several freeze–thaw cycles and heated at 60 °C. After 8 h, a solution of 100 mg of AIBN in 5 mL of dry THF was added in several fractions to the reaction mixture, which was allowed to react at 60 °C for further 7 h. The reaction was finally stopped by adding methanol and the solvent evaporated under reduced pressure.

The obtained solid material was dissolved in chloroform and fractionated by column chromatography (B-685 Medium Pressure, SiO_2 30–60 μm) initially with $CHCl_3$ (collecting nine fractions) and then with $CHCl_3$/MeOH 9:1 v/v (collecting three final fractions) as eluent (Table 2).

2.6. Cobalt mediated polymerization of (S)-MAP in the presence of AIBN

Several reaction mixtures [500 mg of monomer, 2% weight of AIBN, 7.5 mL of dry THF and known amount of Co(II)(DHIB–BF_2)$_2$(H_2O)$_2$ as chain transfer catalyst] were introduced into the vials under nitrogen atmosphere, submitted to several freeze–thaw cycles and heated at 60 °C for 6 h. The reactions were stopped by pouring the mixture into a large excess of methanol and the coagulated polymers filtered off. The solid products were repeatedly redissolved in THF and precipitated again in methanol/hexane 3:1 v/v. The materials were finally dried at 60 °C under vacuum for several days to constant weight.

Relevant data for the synthesized samples are reported in Table 3.

Table 2
Characterization data of samples of poly[(*S*)-MAP] obtained by free radical polymerization followed by fractionation by column chromatography in $CHCl_3$ then $CHCl_3$/MeOH 9:1 v/v

Samples	$\bar{M}_{n\ SEC}$ [a] (g/mol)	$\bar{M}_w/\bar{M}_n$ [a]	$[\alpha]_D^{25}$ [b]	$[\Phi]_D^{25}$ [c]
Poly-17400	17,400	1.39	+381	+1277
Poly-16100	16,100	1.34	+386	+1295
Poly-14400	14,400	1.30	+362	+1214
Poly-12400	12,400	1.28	+377	+1266
Poly-10900	10,900	1.41	+344	+1153
Poly-10100	10,100	1.34	+356	+1194
Poly-9100	9100	1.33	+322	+1081
Poly-8800	8800	1.40	+300	+1005
Poly-5900	5900	1.31	+289	+969
Poly-8900[d]	8900	1.64	+300	+1008
Poly-8500[d]	8500	1.77	+296	+994
Poly-13300[d]	13,300	2.18	+350	+1175

[a] Determined by SEC in THF at 25 °C.
[b] Specific optical rotation, expressed as deg dm^{-1} g^{-1} dL.
[c] Molar optical rotation, expressed as deg dm^{-1} mol^{-1} dL and calculated as ($[\alpha]_D^{25}M$/100), where *M* represents the molecular weight of one repeating unit of poly[(*S*)-MAP].
[d] Eluted with $CHCl_3$/MeOH 9:1 v/v.

Table 3
Characterization data of samples of poly[(*S*)-MAP] obtained by cobalt mediated polymerization

Samples	Chain transfer (mol/L)	Monomer conversion (%)[a]	$\bar{M}_{n\ SEC}$[b] (g/mol)	$\bar{M}_w/\bar{M}_n$[b]	T_g (°C)[c]	$[\alpha]_D^{25}$[d]	$[\Phi]_D^{25}$[e]
Poly-4600	3.17×10^{-5}	6.8	4600	2.00	120	+300	+1004
Poly-15600	3.39×10^{-6}	22.1	15,600	1.77	155	+409	+1373
Poly-23200	3.17×10^{-7}	31.2	23,200	1.75	165	+420	+1409
Poly[(*S*)-MAP][f]	–	69	31,500	1.6	169	+410	+1374

[a] Calculated as (grams of polymer/grams of monomer) 100.
[b] Determined by SEC in THF at 25 °C.
[c] Determined by DSC, heating rate of 10 °C/min under nitrogen atmosphere.
[d] Specific optical rotation, expressed as deg dm^{-1} g^{-1} dL.
[e] Molar optical rotation, expressed as deg dm^{-1} mol^{-1} dL and calculated as ($[\alpha]_D^{25}M/100$), where M represents the molecular weight of one repeating unit of poly[(*S*)-MAP].
[f] Ref. [12], obtained by free radical polymerization by using AIBN as thermal initiator.

3. Results and discussion

3.1. Synthesis and characterization of the oligomeric models

MMA oligomers have been obtained by a similar procedure to those reported in the literature [17,20,21] by fractional distillation of the crude product achieved by radical polymerization of MMA in the presence of AIBN as thermal initiator and $[Co(II)DDDD\text{-}H]^+CH_3COO^-$ as chain transfer agent. Then, they have been hydrolyzed in the presence of an excess of KOH in absolute ethanol to give the corresponding methacrylic acid oligomers (MA acid oligomers) in high yield (Scheme 1). The MA acid dimer and trimer have been recently reported as obtained by selective alkaline hydrolysis in water of the related MMA oligomers after 16 h reaction [22]. By using ethanol as solvent, instead, we have been able to obtain the desired products in about 1 h, in quantitative yield. The MA acid tetramer is a novel product and has been fully characterized by FT-IR, ^1H and ^{13}C NMR (Section 2).

The oligomeric acid derivatives have been finally esterified at room temperature with the azoic alcohol (*S*)-HAP in the presence of DIPC and DPTS as coupling agent and catalyst [23], respectively (Scheme 1).

The chemical structures of the obtained products have been confirmed by FT-IR, ^1H and ^{13}C NMR spectra. As reported in Fig. 3, the ^1H NMR spectrum of (*S*)-MAP dimer shows a singlet at 2.60 related to the methylenic protons of the C3 atom of the backbone (B_3), the trimer and the tetramer exhibit, in the range 1.80–2.60 ppm, also signals related to B_5 and B_7, respectively. In the region close to 1.10 ppm, the resonances related to methyl protons, whose number increases by passing from dimer to tetramer, are present.

As reported in Table 1, the yields of methacrylic oligomers decrease from (*S*)-MAP dimer to the tetramer as a consequence of the possibility of intramolecular formation of cyclic anhydride derived by condensation between two neighbouring acid groups, and the decreasing reactivity of the oligomeric acid substrate, due to steric hindrance of the produced azoic ester towards further functionalization. Such a behaviour rules out the possibility to obtain higher methacrylic oligomers by this synthetic pathway. Thus, we have resolved to obtain them by direct radical polymerization of monomer (*S*)-MAP under conditions favouring the formation of macromolecular derivatives of low average molecular mass.

3.2. Preparation, fractionation and characterization of poly[(S)-MAP] samples of different average molecular weight

Free radical polymerization of (*S*)-MAP was carried out in the presence of a large excess of AIBN (10% wt with respect to

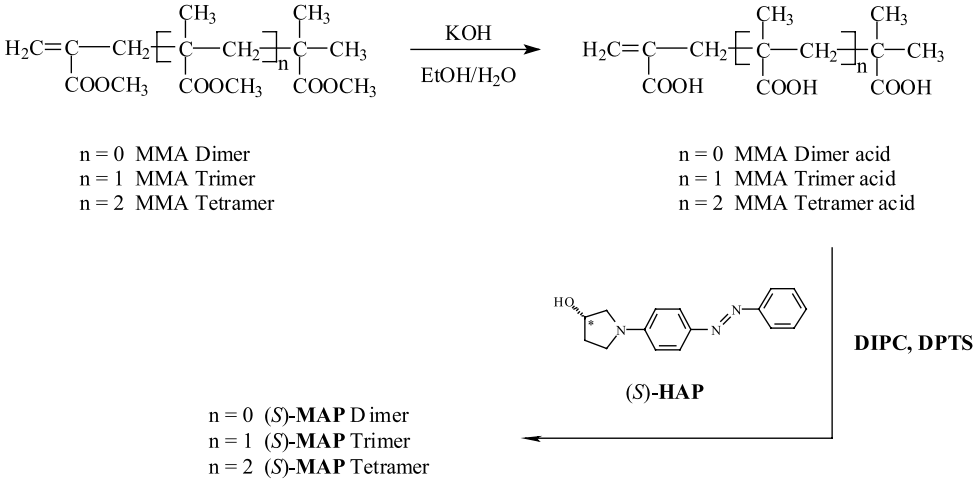

Scheme 1.

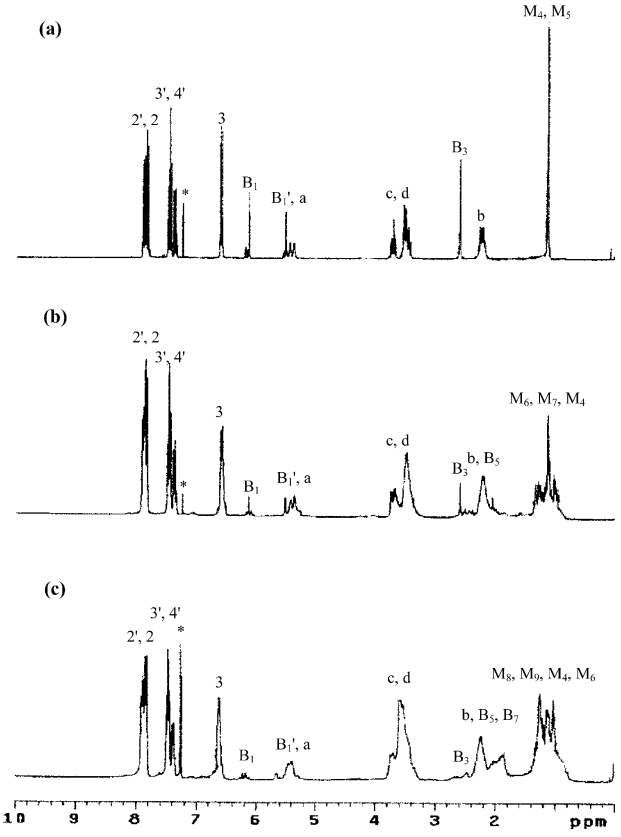

Fig. 3. ^{1}H NMR spectra in $CDCl_3$ of (a) (*S*)-MAP dimer, (b) (*S*)-MAP trimer and (c) (*S*)-MAP tetramer. Starred signals refer to solvent resonances.

the monomer) with the aim to obtain a polymeric derivative with higher polydispersity index and lower average molecular weight than that one formerly obtained using 2% weight of radical initiator [12] ($\bar{M}_n = 31{,}500$ g/mol with a polydispersity index of 1.6).

Subsequent fractionation of the crude product by column chromatography, allowed us to achieve samples with various average polymerization degree, as reported in Table 2. A similar fractionation was successfully performed by Green and co-workers for polydisperse polyisocyanate samples by using an analytical gel permeation chromatography apparatus [24].

To obtain macromolecules with low average molecular weight, the radical polymerization was carried out also in the presence of a cobalt complex as chain transfer agent. This latter, in fact, if added in suitable amounts, can be used to control the increase of molecular weight because of its capability to transfer the activation centre of polymerization from one molecule to another one. Thus, as reported by Janowicz [17,18] in particular for the homopolymerization of methyl methacrylate, changing the concentration of Co(II)(DHIB–BF_2)$_2$(H_2O)$_2$ [18] in the reaction mixture, allowed us to obtain macromolecules with various chain length (Table 3). Cobalt mediated polymerization, however, did not allow to lower the molecular weight distribution, which resulted relatively high (in the range 1.75–2.00) (Table 3) if compared with those of the samples previously obtained by ATRP (1.2–1.3) [15] and by free radical polymerization with AIBN 2% only (about 1.6) [12].

All the obtained derivatives, characterized by FT-IR, ^{1}H and ^{13}C NMR, show spectra in accordance with the expected structure for poly[(*S*)-MAP] [12].

In particular, the band at 1634 cm^{-1}, related to the stretching vibration of the double bond in the monomer was absent in the FT-IR spectra, and the estereal carbonyl stretching frequency moved from 1709 cm^{-1} in the monomer to higher frequency (1729 cm^{-1}) in the polymer, due to the reduced electron delocalization, determined by the reaction of the methacrylic double bond. Accordingly, in the ^{1}H NMR spectra of all polymeric samples, the resonances at 5.60 and 6.10 ppm, related to the vinylidenic protons of monomer (*S*)-MAP, were absent and the methyl resonances are shifted from about 1.95 ppm to higher field.

Due to the relatively higher average molecular weight with respect to the homopolymers previously obtained by ATRP [15] no relevant signals related to the AIBN initiator and to other possible end-groups are visible in the ^{1}H and ^{13}C NMR spectra.

The thermal stability of all polymeric samples, as determined by thermogravimetric analysis (TGA), are rather high, with values of initial decomposition in air ranging around 300 °C, indicative of the presence of strong dipolar interactions between azobenzene chromophores in the side-chain, which appear to be independent from the $\bar{X}_n$ and $\bar{M}_w/\bar{M}_n$ values. The DSC analysis shows only second order thermal transitions related to glass transitions, in accordance with the amorphous character of these polymers. As previously reported [15], the polymeric derivatives obtained by ATRP show T_g values, which increase from about 122 to 160 °C upon increasing the average molecular weight, thus approaching the 169 °C value found for poly[(*S*)-MAP] obtained by AIBN initiated free radical polymerization [12]. The same behaviour is shown by the samples obtained by free radical polymerization in the presence of cobalt complex (Table 3), their T_g values resulting lower because of higher polydispersity.

Both the good thermal stability and high values of T_g suggest that these polymeric systems, although possessing low average molecular weight and high polydispersity, may be promising for solid state applications in opto-electronics due to their stability at room temperature subsequently to photo- or electrically induced orientation of the azoaromatic dipoles. In addition, the wide range of average polymerization degree ($13 < \bar{X}_n < 70$) and molecular weight distribution of the obtained samples of poly[(*S*)-MAP] (Tables 2 and 3), gives the possibility to observe the dependence of their properties on the average chain length.

3.3. UV–vis properties

The UV–vis spectra of the oligomeric models (Table 4), as well as those one of all polymeric derivatives, display in dilute $CHCl_3$ solution, in the 250–700 nm spectral region, two absorption bands centered at around 408 and 258 nm. The former one, more intense, is attributed to electronic transitions

Table 4
UV–vis spectra in $CHCl_3$ solution at 25 °C of model (*S*)-PAP, (*S*)-MAP oligomers and poly[(*S*)-MAP]

Samples	1st Band		2nd Band	
	λ_{max} [a]	$\varepsilon_{max} \times 10^{-3}$ [b]	λ_{max} [a]	$\varepsilon_{max} \times 10^{-3}$ [b]
(*S*)-PAP[c]	409	29.8	258	11.6
(*S*)-MAP dimer	408	27.3	261	10.2
(*S*)-MAP trimer	407	27.2	258	10.3
(*S*)-MAP tetramer	408	27.0	258	10.6
Poly[(*S*)-MAP][c]	408	28.3	258	10.5

[a] Wave length of maximum absorbance, expressed in nanometers.
[b] Expressed in L mol^{-1} cm^{-1} and calculated for one single chromophore.
[c] Ref. [12].

such as n–π^*, π–π^* and internal charge transfer of the azobenzene chromophore; the latter to the π–π^* electronic transition of aromatic ring [25]. These bands are similar to those previously reported for poly[(*S*)-MAP] [12], with no apparent dependence on the amount of side-chain chromophores present in the samples examined, as recently also observed for the analogous derivatives obtained by ATRP [15].

A significant hypochromism, for both the first and the second band, was displayed passing from the model (*S*)-PAP to the related polymer poly[(*S*)-MAP] [12], regardless the solvent employed. Such a behaviour, frequently noticed in polymers bearing side-chain aromatic chromophores [26–28], is attributed to the occurrence of electrostatic dipole-dipole interactions between the neighbouring aromatic chromophores [29–31]. As shown in Table 4, the molar absorption coefficient values of one single chromophore, related to the first absorption band of (*S*)-MAP oligomers, result lower than those given by the model compound (*S*)-PAP and even by poly[(*S*)-MAP] having $\bar{M}_n = 31{,}500$ g/mol. It appears, therefore, that dipolar interactions between few chromophoric units in the oligomeric models are able to give rise to a larger hypochromic effect with respect to that given by the polymeric derivatives.

3.4. Optical activity, CD spectra and chiroptical properties

With the aim to study the dependence of the optical activity on the average molecular weight of these materials, the specific $\{[\alpha]_D^{25}\}$ and molar $\{[\Phi]_D^{25}\}$ optical rotation of the oligomeric compounds and the polymeric derivatives have been determined in $CHCl_3$ solution at the sodium D line (Tables 1–3). As reported in Table 1, all oligomeric products show molar optical rotation values higher than the model compound (*S*)-PAP, which increase in each molecule with the enhancement of the number of chiral residues of (*S*)-3-hydroxy pyrrolidine or, in other words, with the increase of $\bar{X}_n$. This behaviour suggests that few adjacent chiral units are able to produce a remarkable increase of the optical activity of these derivatives.

The molar optical rotation values plotted versus the average polymerization degree of samples obtained by different procedures in previous and in the present work, are reported in Fig. 4, exception made for the samples obtained by chromatographic elution with $CHCl_3$/MeOH 9:1 v/v

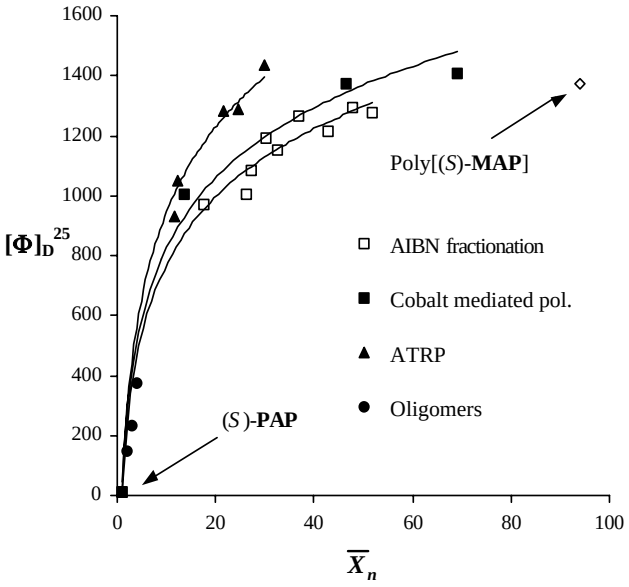

Fig. 4. Evolution of molar optical rotation, $[\Phi]_D^{25}$ versus the average number polymerization degree determined by SEC, relative to the oligomeric derivatives (●) and the polymeric samples of poly[(*S*)-MAP] obtained by free radical polymerization with AIBN (□), cobalt mediated polymerization (■) and ATRP [15] (▲). The values for (*S*)-PAP and poly[(*S*)-MAP] with $\bar{M}_n = 31{,}500$ from Ref. [12] are also reported.

(Table 2), as their higher polydispersity index (1.7–2.2) with respect to those shown by the fractions eluted with $CHCl_3$ only (1.2–1.4) precludes an univocal correlation of $[\Phi]_D^{25}$ to a specific value of $\bar{X}_n$. It can be in fact noticed that, depending on the synthetic method adopted, slightly different trends are obtained, the values of molar optical rotation being in any case non linear with the average molecular weight. Considering the non-symmetric molecular weight distribution in each sample, with a longer tail at molecular weights lower than the average, the polymers with the same $\bar{M}_n$ but different polydispersity will behave differently, with inferior chiroptical properties for the system containing more amount of oligomeric component. Indeed, the samples previously obtained by ATRP [15], which are characterized by a lower molecular weight distribution (1.2–1.3), show higher values of $[\Phi]_D^{25}$, whereas the polymeric derivatives obtained in the presence of chain transfer agent ($\bar{M}_w/\bar{M}_n$ 1.8–2.0) show lower optical activity (Fig. 3 and Table 2).

All the curves reported in Fig. 4 display similar trends, thus evidencing analogous dependence of $[\Phi]_D^{25}$ on the average molecular weight of the macromolecules examined. In general, the optical activity increases rapidly in the range $\bar{X}_n = 1$–15, then tends to level off at a constant value, which is achieved for $\bar{X}_n < 20$–25. A similar trend of optical rotation versus the average polymerization degree was reported by Teramoto [32] for chiral polyisocyanates, but only for $\bar{X}_n$ values ranging from above 400 to 1000. This finding was attributed to helix conformation of the main chain forced by the increase of molecular weight and stiffness.

The remarkable contribution of the macromolecular chain length to optical activity could be due, in principle, to conformational and/or configurational effects originated by

Table 5
CD spectra in $CHCl_3$ solution at 25 °C of (*S*)-MAP oligomers and selected samples of poly[(*S*)-MAP]

Samples	1st Absorption band					2nd Absorption band	
	λ_1[a]	$\Delta\varepsilon_1$[b]	λ_0[c]	λ_2[a]	$\Delta\varepsilon_2$[b]	λ_3[a]	$\Delta\varepsilon_3$[b]
(*S*)-PAP[d]	410	−0.51	–	–	–	258	+0.22
(*S*)-MAP dimer	427	+0.58	398	380	−0.34	n.d.	n.d.
(*S*)-MAP trimer	432	+0.94	402	384	−0.46	n.d.	n.d.
(*S*)-MAP tetramer	431	+1.41	402	381	−0.71	n.d.	n.d.
Poly-17400	448	+6.98	410	386	−5.32	258	−0.52
Poly-16100	446	+6.27	410	386	−4.93	259	−0.35
Poly-14400	448	+6.57	410	386	−4.69	258	−0.48
Poly-10100	447	+5.42	409	383	−4.96	259	−0.22
Poly-8800	448	+5.72	410	387	−4.12	255	−0.42
Poly-13300[e]	448	+5.90	410	386	−4.49	259	−0.38
Poly-4600[f]	444	+4.70	408	385	−3.50	258	−0.25
Poly-15600[f]	444	+6.18	410	385	−5.56	258	−0.35
Poly-23200[f]	445	+6.81	411	386	−6.27	260	−0.32
Poly[(*S*)-MAP][d]	445	+7.35	409	387	−6.42	258	−0.32

[a] Wavelength (in nm) of maximum dichroic absorption.
[b] $\Delta\varepsilon$ expressed in L mol^{-1} cm^{-1} and calculated for one repeating unit in the polymer.
[c] Wave length (in nm) of the cross-over of dichroic bands.
[d] Ref. [12].
[e] Obtained by chromatographic fractionation with $CHCl_3$/MeOH 9:1 v/v.
[f] Obtained by cobalt mediated polymerization.

a prevalent tacticity of the polymeric backbone. An evaluation of the microtacticity can be made by ^{13}C NMR analysis of the signals originated by the methacrylic methyl group, which displays two resonances located at ≈19.8 and 17.5 ppm, assigned to mr (meso–racemo) and rr (racemo–racemo) heterotactic and syndiotactic triads, respectively [33]. Integration of these resonances allows to establish that the main chain microstructure of the polymeric derivatives is essentially atactic, with a predominance of syndiotactic triads (rr = 46–55%), which is quite close to the values obtained for the derivatives previously obtained with other procedures [12,15]. It can be therefore stated that the relevant optical activity of these materials is essentially of conformational origin, rather than related to the presence of a predominant configuration of the stereogenic centres in the main chain, in line with previous results obtained for analogous homopolymeric derivatives bearing in the side-chain strongly conjugated azoaromatic chromophores [11,13]. Furthermore, the results confirm the hypothesis that the optical activity of these materials should be substantially related to relatively short chain sections with conformational dissymmetry of one prevailing screw sense.

To investigate in detail the chiroptical properties, the (*S*)-MAP oligomers and some selected polymeric derivatives have been submitted to CD spectroscopy in chloroform solution in the spectral region between 250 and 700 nm (Table 5, Figs. 5 and 6).

By contrast with model (*S*)-PAP [12], displaying only weak negative and positive signals (Table 5 and Fig. 5) in correspondence of the UV–vis absorptions related to the first and the second absorption band, respectively, the CD spectra of all the obtained derivatives exhibit, in the spectral region connected to the first UV–vis band, two strong dichroic signals of opposite sign with cross-over points close to the UV maximum absorption at about 408 nm. Such a behaviour is typical of an exciton splitting determined by co-operative dipolar interactions between the neighbouring side-chain optically active azoaromatic chromophores disposed in a mutual chiral geometry of one prevailing handedness along the polymeric chain [1,10,14,34]. In the spectral region connected to the second UV–vis band, instead, a weak negative dichroic band at 258 nm is present.

As shown in Fig. 5, the chiral interactions between one couple of chromophores only, in solution are already important, the CD spectrum of (*S*)-MAP dimer displaying a significant exciton couplet. The couplet increases then progressively its amplitude upon increasing the chain length, the polymeric derivatives displaying correspondingly higher

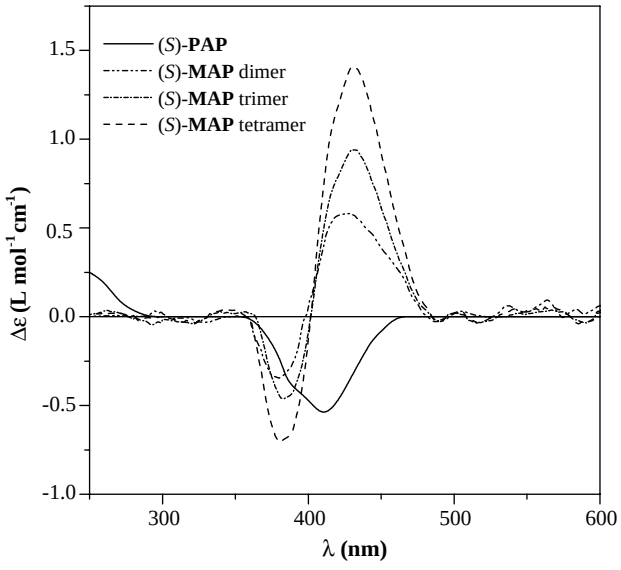

Fig. 5. CD spectra of the oligomeric derivatives in $CHCl_3$ solution.

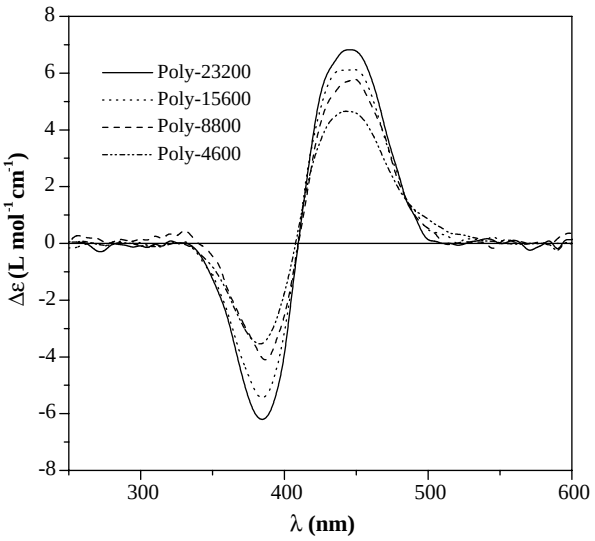

Fig. 6. CD spectra of selected polymeric derivatives with different average molecular weight in $CHCl_3$ solution.

dichroic signals, with a tendency to reach a maximum amplitude at the highest molecular mass values (Fig. 6).

To evaluate the amount of dissymmetric conformations assumed by the macromolecules in chloroform solution, we report in Fig. 7 the integrated areas of the dichroic bands connected to the first UV–vis absorption band as a function of the average polymerization degree of the synthesized compounds and the recently reported derivatives obtained by ATRP [15]. It appears that the CD signals are strongly dependent on the average molecular weight, the maximum value being roughly corresponding to a $\bar{X}_n$ value of 20–25, after which it remains approximately constant, in agreement with the results obtained by polarimetry.

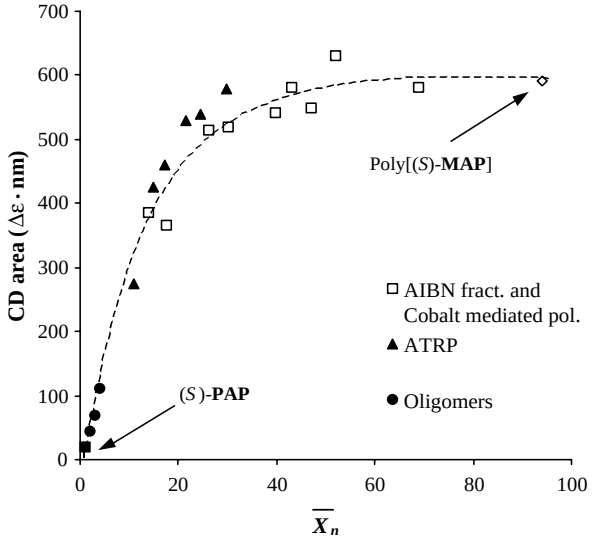

Fig. 7. Evolution of the amplitude of the CD exciton couplet versus the average number polymerization degree calculated by SEC, relative to the oligomeric derivatives (●) and the polymeric samples of poly[(*S*)-MAP] obtained by free radical polymerization with AIBN or cobalt mediated polymerization (□) and ATRP [15] (▲). The values for (*S*)-PAP and poly[(*S*)-MAP] with $\bar{M}_n = 31{,}500$ from Ref. [12] are also reported.

This behaviour could be simply explained with the usual model of electrostatic dipolar interchromophore interactions adopted to describe the CD spectra [34–36]. In fact, the chiroptical properties of interacting chromophores are strongly affected by their dihedral angle and relative distance (R) (by a factor of about $1/R^6$). When in the polymer the number of repeating units increases, their relative distance R also increases and consequently the interactions of one chromophore are progressively decaying on passing from the adjacent, to the third one, the fourth chromophore and so forth, with convergence of the intensity of the CD signals to one asymptotic value.

4. Conclusions

Well defined oligomeric compounds (dimer, trimer and tetramer) as well as a series of samples of optically active photochromic methacrylic polymers in a wide range of average polymerization degree ($13 < \bar{X}_n < 70$) with different molecular weight distributions, have been synthesized to investigate model systems displaying increasing interchromophore interactions in chiral azo-polymers. The glass transition temperatures of polymeric derivatives result to depend on the average molecular weights and their distribution: at values of $\bar{M}_n = 23200$ and polydispersity of 1.75 the transition takes place at 165 °C. This high value of T_g, originated by the presence of strong polar interactions between chromophores in the solid state, is promising for technological applications in micro- and opto-electronics.

The optical activity of all polymeric derivatives results to be much higher that those of monomer and low molecular weight model compound and is highly dependent on their average molecular weight and polydispersity, especially at low values of polymerization degree. Both the molar optical rotation values and CD bands rise rapidly in the range $\bar{X}_n = 1$–15, then they approach an asymptotic value, which is achieved for $\bar{X}_n > 20$–25, slightly affected by the further increase of molecular weight.

The CD spectra of the oligomeric models display approximately the same shape as the related polymers, with reduced intensity: the dimeric compound exhibiting about one tenth, the trimer one sixth and the tetramer one fourth of the maximum CD intensity in the polymers. Such a behaviour confirms that the contribution to the overall optical activity given by the interactions between chromophores having conformational dissymmetry of one prevailing screw sense, is already relevant for short chain sections, as theorized in a previous detailed investigation on the spectroscopic and chiroptical properties of a similar dimeric derivative containing two photochromic chiral moieties.

Acknowledgements

The financial support by MIUR (PRIN2004) and Consortium INSTM (FIRB2001 'RBNE01P4JF') is gratefully acknowledged.

References

[1] Carlini C, Angiolini L, Caretti D. Photocromic optically active polymers. Polymeric materials encyclopedia, vol. 7. Boca Raton: CRC Press; 1996. p. 5116.
[2] Proceedings of the symposium on azobenzene-containing materials, Boston MA (USA) 1998. A. Natansohn, editor. Macromolecular symposia 137; 1999. p. 1–165.
[3] Verbiest T, Kauranen M, Persoons A. J Mater Chem 1999;9:2005.
[4] Hopkins TE, Wagener KB. Adv Mater 2002;14:1703.
[5] Xie S, Natansohn A, Rochon P. Chem Mater 1995;5:403.
[6] Angiolini L, Bozio R, Giorgini L, Pedron D, Turco G, Daurù A. Chem Eur J 2002;8:4241.
[7] Angiolini L, Benelli T, Bozio R, Daurù A, Giorgini L, Pedron D. Synth Met 2003;139:743.
[8] Angiolini L, Caretti D, Giorgini L, Salatelli E, Altomare A, Carlini C, et al. Polymer 1998;39:6621.
[9] Angiolini L, Caretti D, Carlini C, Salatelli E. Macromol Chem Phys 1995; 196:2737.
[10] Angiolini L, Caretti D, Giorgini L, Salatelli E. Macromol Chem Phys 2000;201:533.
[11] Angiolini L, Caretti D, Giorgini L, Salatelli E. Polymer 2001;42:4005.
[12] Angiolini L, Caretti D, Giorgini L, Salatelli E. J Polym Sci, Part A: Polym Chem 1999;37:3257.
[13] Angiolini L, Caretti D, Giorgini L, Salatelli E. e-Polymers 2001;021.
[14] Painelli A, Terenziani F, Angiolini L, Benelli T, Giorgini L. Chem Eur J 2005;11:6053.
[15] Angiolini L, Benelli T, Giorgini L, Salatelli E. Polymer 2005;46:2424.
[16] Perrin DD, Amarego WLF, Perrin DR. Purification of laboratory chemicals. Oxford: Pergamon Press; 1966.
[17] Janowicz AH, Melby LR. US Patent 4,680,352; 1987.
[18] Janowicz AH. US Patent 4,694,054; 1987.
[19] Bakac A, Espenson JM. J Am Chem Soc 1984;106:5197.
[20] Moad CL, Moad G, Rizzardo E, Thang SH. Macromolecules 1996;29: 7717–26.
[21] McCord E, Anton WL, Wilczek L, Ittel SD, Nelson LTJ, Raffell KD. Macromol Symp 1994;86:47.
[22] Hutson L, Krstina J, Moad CL, Moad G, Morrow GR, Postma A, et al. Macromolecules 2004;37(12):4441–52.
[23] Moore JS, Stupp S. Macromolecules 1990;23:65.
[24] Jha SK, Cheon K, Green MM, Selinger JV. J Am Chem Soc 1999; 121:1665.
[25] Altomare A, Ciardelli F, Ghiloni MS, Solaro R, Tirelli N. Macromol Chem Phys 1997;198:1739.
[26] Chiellini E, Solaro R, Galli G, Ledwith A. Macromolecules 1980;13: 1654.
[27] Majumdar RN, Carlini C. Makromol Chem 1980;181:201.
[28] Carlini C, Gurzoni F. Polymer 1983;24:101.
[29] Tinoco Jr I. J Am Chem Soc 1960;82:4785.
[30] Okamoto K, Itaya A, Kusabayashi S. Chem Lett 1974;1167.
[31] Ciardelli F, Aglietto M, Carlini C, Chiellini E, Solaro R. Pure Appl Chem 1982;54:521.
[32] Teramoto A. Prog Polym Sci 2001;26:667–720 and references therein.
[33] Peat IR, Reynolds WF. Tetrahedron Lett 1972;1359.
[34] Rodger A, Nordén B. Circular dichroism, and linear dichroism. Oxford: Oxford University Press; 1997 [chapters 5 and 7].
[35] Mason SF. Molecular optical activity and the chiral discrimination. Cambridge: Cambridge University Press; 1982 [chapter 3].
[36] Berova N, Nakanishi K, Woody RW. Circular dichroism, principles and applications. New York: Wiley–VCH; 2000.